Original Research Article

Estimation of rice crop acreage in Kuttanad Region, Kerala using Landsat 8 OLI IMAGES and GIS Techniques

Abstract

Aims: The study aimed to delineate rice accurately (*Oryza sativa L.*) cultivation areas in the Kuttanad region, Kerala, during the *Puncha* season of 2023-24 using medium- to high-resolution optical satellite data, particularly Landsat 8 Operational Land Imager (OLI), to aid in preharvest prediction of agricultural production and policy making

Study design: This study used a remote sensing-based approach for rice area estimation, focusing on supervised classification methods.

Place and Duration of Study: The study was conducted in Kuttanad, Kerala, a low-lying agroecosystem, during the *Puncha* season of 2023-24.

Methodology: The study utilised two cloud-free Landsat 8 OLI images for the delineation of rice-growing areas. The images were pre-processed, mosaicked, and analysed using ArcGIS software. A supervised classification approach was employed using the Maximum Likelihood Classification algorithm. The study area was classified into five categories: rice fields, other crops, low vegetation, built-up areas, and water bodies. Ground-truth data was used to validate the classification accuracy.

Results: The total rice area delineated during the *Puncha* season was 43,550.28 hectares. The classification achieved an accuracy of 93.33%, with a kappa coefficient of 0.87, indicating high reliability.

Conclusion: The accurate delineation of rice-growing areas using satellite imagery provides valuable information for assessing production levels and planning for food security. This methodology can aid in agricultural planning and contingency strategies, particularly in regions like Kuttanad, which face challenges such as flooding and soil toxicity

Keywords: Optical Remote Sensing, Rice area estimation, Landsat 8 OLI IMAGES, Supervised classification

Introduction

Over 50% of the world's population depends primarily on rice (*Oryza sativa L.*), which is grown on around 140 million hectares of land (Khush, 2005). According to predictions made by Yuan *et al.,* (2021) there will be a significant increase in the amount of rice consumed worldwide by 2030, from 480 million tons of milled rice in 2014. India plays a critical role in both national and international food security, producing 21% of the world's rice (130.29 million tons yearly) from an area of 46.38 million hectares (GOI, 2023). The Green Revolution was crucial in raising rice yield, production, and crop density and expanding rice cultivation areas in India to meet the demands of a growing population (Matsumura *et al.,* 2009). However, challenges such as urbanisation, the shift to cash crops, and decreasing labour availability threaten the preservation of rice acreage in India. Kerala witnessed an abrupt decrease in the area used for rice cultivation from 8.7 lakh hectares in 1970–1971 to 1.96 lakh hectares in 2021–2022, which led to a 90% drop in output (Agricultural Statistics 2021-22). Climate variability, especially changes in

temperature and rainfall, can affect rice yields because rice requires more water than other crops (Ahmed and Ahmad, 2017). Thus, developing import and export strategies to meet production deficits or surpluses requires accurate pre-harvest rice yield forecasting based on the previous year's vegetation conditions (Huang *et al.*, 2002; Nuarsa *et al.*, 2012).

The primary source of information for rice mapping in the 1980s and early 1990s was regularly updated agricultural statistical data (Huke and Huke, 1997). However, recent advancements in remote sensing technology have provided a reliable alternative for estimating large-scale crop acreage (Yang, 2007; Chen, 2007; Koppe *et al.*, 2013).

Remote sensing offers numerous advantages, such as broad spatial coverage, year-round availability, and cost-effectiveness due to the freely accessible optical images from MODIS, IRS LISS-III, Landsat and Sentinel. The availability of contemporary high-resolution satellite images has significantly improved crop yield forecast, crop differentiation, crop planting area calculation, and crop growth modelling (Bolton and Friedl, 2013; Mondal *et al.*, 2014; Singha *et al.*, 2019). Rice mapping has successfully made use of satellite data with both mono- and multi-temporal inputs. Mono-temporal image data can be particularly useful for identifying rice fields, as obtaining cloud-free images during the rice growing season is often challenging. Many researchers have made notable contributions to this field.

Recently, several studies have successfully mapped rice cultivation areas using phenology-based algorithms and various multi-temporal images, including LANDSAT (Dong *et al.*, 2016; Hedayati *et al.*, 2022), IRS LISS-III (Mondal *et al.*, 2014), MODIS (Zhang *et al.*, 2017; Jiang *et al.*, 2018), Sentinel-1 (Mansaray *et al.*, 2019; , Shen and Nie, 2023), and Sentinel-2 (Raju *et al.*, 2022) at both global and regional scales.

Karydas et al. (2015) developed a rule-based method for mapping rice cultivation using Landsat 8 time series data for the plains of Thessaloniki, Greece. Genc et al. (2014) developed land use and land cover maps for Biga town after classifying Landsat data into six categories to identify paddy fields. Yedage et al. (2013) focused on identifying and evaluating pomegranate crop zones in Maharashtra using IRS P6 and LANDSAT-7 data. Using cloud-free, single-date Resourcesat-1 LISS-III digital data that coincided with the wheat blossoming stage, Goswami et al. (2012) calculated the acreage. Three multi-temporal, cloud-free Sentinel-2 datasets were utilized by Raju et al. (2022) to map rice areas in the Palakkad district of Kerala.

While Ajith *et al.*, (2017) estimated the amount of rice acreage in Tamil Nadu using Landsat 8 OLI data, *Persello et al.*, (2019) used MODIS NDVI data to map rice regions in Bangladesh. Compared to MODIS imagery, Landsat images have a higher geographical and temporal resolution (16-day repeat), making them more potentially useful for identifying paddy fields (Wang *et al.*, 2015). In addition to Landsat 5 and 7, Landsat 8 pictures provide enhanced precision for LULC mapping and assessment (Roy *et al.*, 2014). Additionally, Landsat 8 provides advances in radiometric, spectral, and geographic resolution, and daily imagery is possible (Roy *et al.*, 2014).

The goal of the study is to assess how well medium- to high-resolution optical satellite data, particularly the Landsat 8 OLI, can map the regions used for rice

farming in the Kuttanad region of Kerala during the 2023–

2024 *Puncha* season. Since the cloud cover is a major challenge during rice cultivation season, assessing the potential of freely available optical satellite images is very important. Studies focussing on the delineation of rice area in the major rice growing tract of Kuttanad is also lacking. Information of areas under rice well in advance also helps policymakers to plan regarding food grain availability. Hence the study is carried out to delineate rice area in Kutanad tract. The study hypothesizes that the Landsat 8 time series can effectively capture rice crops, leading to improved resource management and food security strategies.

2. Materials and methods

2.1. Study area

The study was conducted in the (Fig. 1) Kuttanad region of Kerala State, India. Within the districts of Alappuzha, Kottayam, and Pathanamthitta, rice is grown under the unique Kuttanad system, up to three meters below sea level, protected by bunds to prevent inundation of water. The area is located in the southwest of Kerala, between latitudes 7^0 30' to 11^0 15' North and longitudes 75^0 30' to 77^0 30' East. It is bordered on the north, east, west, and south by the districts of Ernakulam, Kottayam, Alappuzha, and Pathanamthitta, respectively. The Kuttanad region known as Kerala's rice bowl and accounts for a significant portion of the state's rice production and receives 2692 mm of rainfall annually. Of this total rainfall, the southwest monsoon, northeast monsoon, summer rains, and winter rains each account for 64.3%, 18.7%, 15.91%, and 1.1% of the total. As the area is low lying most of the paddy fields are under threat of flood water inundation during southwest monsoon period and cultivation is possible during the season only in those areas which have sufficient drainage facilities. Therefore, *Puncha* is the primary crop season, with crops sown in October and November and harvests taking place in February and March. In about one-third of the land where adequate infrastructure for pumping out excess water and suitable drainage facilities are present, an additional crop is also harvested during *Kharif*, which runs from June to September. The study was conducted on the medium-duration *Uma* rice variety in the Kuttanad region during the *Puncha* rice season of 2023–2024.

2.2. Remote Sensing Data

For this study, a 30 m spatial resolution Level 1 product of Landsat 8 Operational Land Imager (OLI) was used. Since two images were required to cover the entire area of Kuttanad, two cloud-free (< 5%) Geo-TIFF images in one path (No. 144) and two rows (Nos. 53 and 54) were obtained as two tiles from https://earthexplorer.usgs.gov/ (Table 1). Fig. 2 shows the acquired raw satellite imagery. The research area's administrative boundaries were superimposed on the pictures to extract the entire pixel that belonged to the region.

2.3. Creating Composite Image from Landsat 8 OLI Imagery

Table 2 provides the band designation for Landsat 8 OLI. Seven of the eleven bands, each with a resolution of 30 m, were combined to make the composite image. Clouds, cloud shadows, haze, and other noisy data might affect individual remote-sensing images. Clearer images that are simpler to compare across time are produced by composite images, which are made by combining many images taken in different bands into one. It is possible to

display images in both true and false color by creating a composite image from several bands. When bands are displayed in RGB, or True Color Composite, images appear

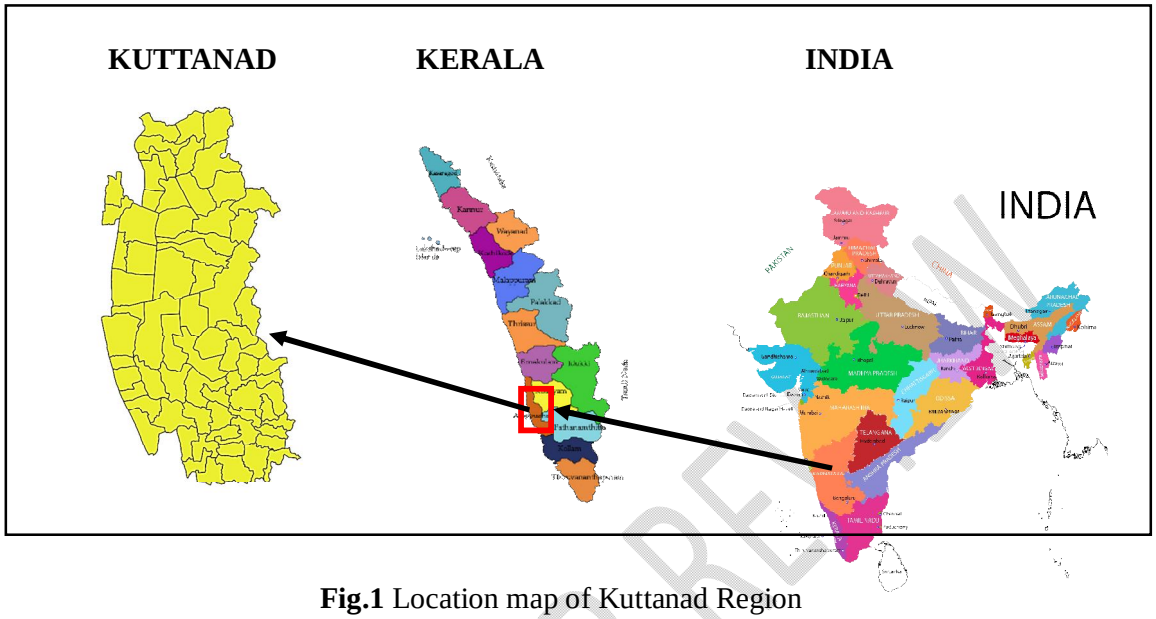

Fig.1 Location map of Kuttanad Region

Table. 1 Landsat 8 OLI images downloaded

Date	Path	Row	Images
22/01/24	144	53	LC08_L1TP_144053_29240122_20240130_02_T1
22/01/24	144	54	LC08_L1TP_144054_29240122_20240130_02_T1

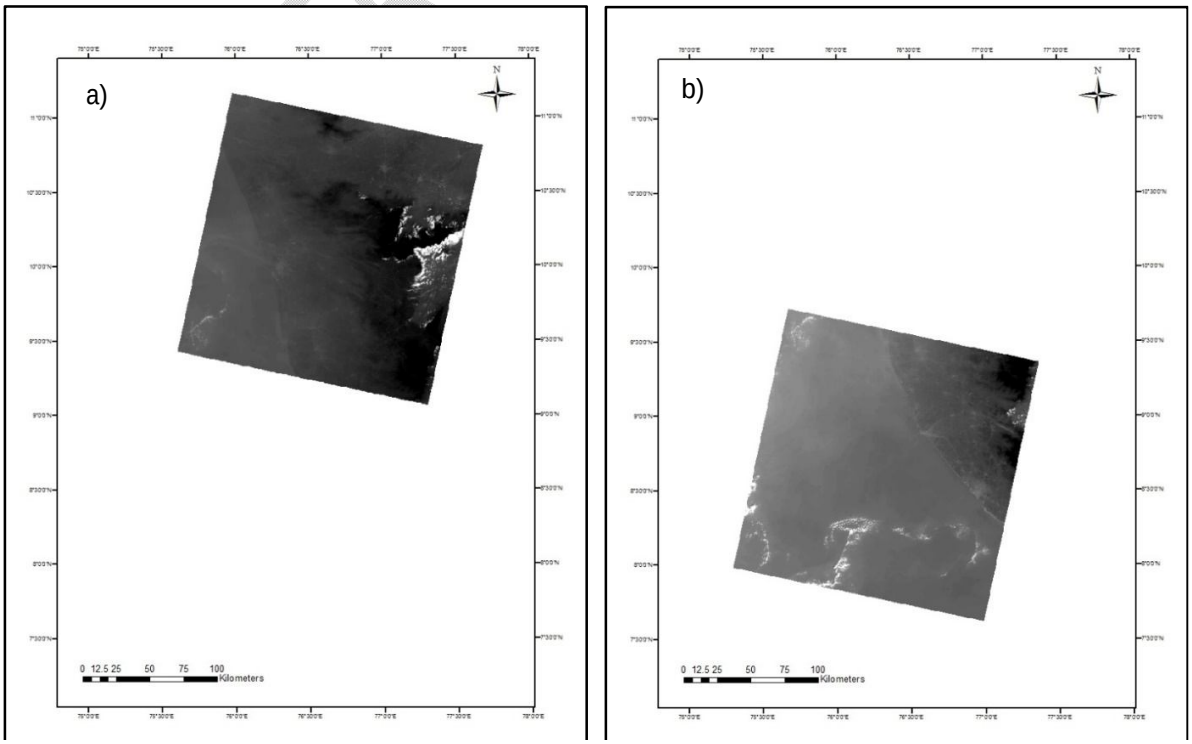

Fig.2 Landsat 8 OLI images of the study area (a. Path 144, Row 53 & b. Path 144, Row 54

more realistic and similar to what the human eye would see. It also helps us recognize various features in a scene and get to know them better, such as identifying cities, forests, agricultural land, and water bodies (Fig. 3). False Colour Composites (FCC) use a colour scheme that helps to identify features like vegetation, clouds, urban areas, and open water in comparison with True Colour Composite and ground truth information. For example, in a false colour image, vegetation with high photosynthetic activity appears bright red, water appears black, and bare ground appears blue or white (Fig 5b). It will be very beneficial to compare true and false colors when performing various studies, including supervised and unsupervised classifications. The Kuttanad region was fully covered by mosaicking images in row 53 and row 54, two neighbouring composite raster datasets (Fig. 4). Combining two raster datasets seamlessly into a single raster image by mosaicking makes categorization simpler. In addition, the mosaic composite image was shown in both True Color (Bands 4,3,2) and False Color (Bands 5,4,3) to facilitate classification. The mosaiked images are then clipped to extract the study region (Fig 5a).

2.4. Maximum Likelihood Classification and rice area estimation

The supervised classification technique was applied using Maximum Likelihood Classification (MLC) provision in ArcGIS10.3 software. Supervised classification is the practicability utilized for quantitative remotely sensed images analysis; it depends on using the proper algorithms to label the image pixels as representing specific classes, or specific land cover types (John and Xiuping, 2006; Miranda, *et al.*, 2018). Maximum likelihood classification (MLC) considers being one of the most widely used supervised classifications in various applications (Erbek, *et al.*, 2004; Muhsin and Kadhim, 2017). A total of 30 rice and 30 non-rice areas were identified in the study area by ground truthing. The spectral signatures were created from these training sites by identifying similar areas and based on this the image was classified in ArcGIS Software. Land use mask available in the Department of Agricultural Meteorology aon RARS, Kumarakom was used for masking the classes with less interest. For this study, a supervised classification method which consisting of five classes

Table.2 Various bands under Landsat 8 OLI

	Bands	Wavelength (micrometers)	Resolution (meters)
Landsat 8 OLI	Band 1 - Ultra Blue	0.43 - 0.45	
	Band 2 – Blue	0.45 - 0.51	30
	Band 3 - Green	0.53 - 0.59	30
	Band 4 - Red	0.64 - 0.67	30
	Band 5 - Near Infrared (NIR)	0.85 - 0.88	30

	Band 6 - Shortwave Infrared (SWIR)	1 1.57 - 1.65	30
	Band 7 - Shortwave Infrared (SWIR)	2 2.11 - 2.29	30

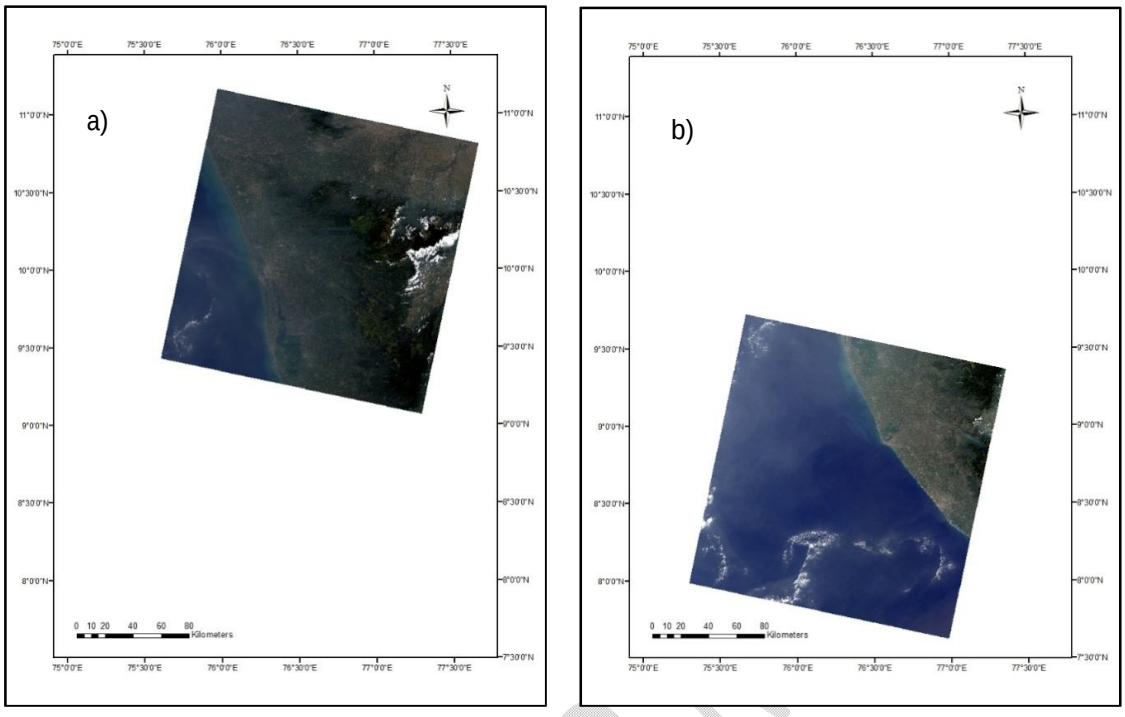

.

Fig.3 True Colour Composite in RGB in rows 53 (3a) and 54 (3b

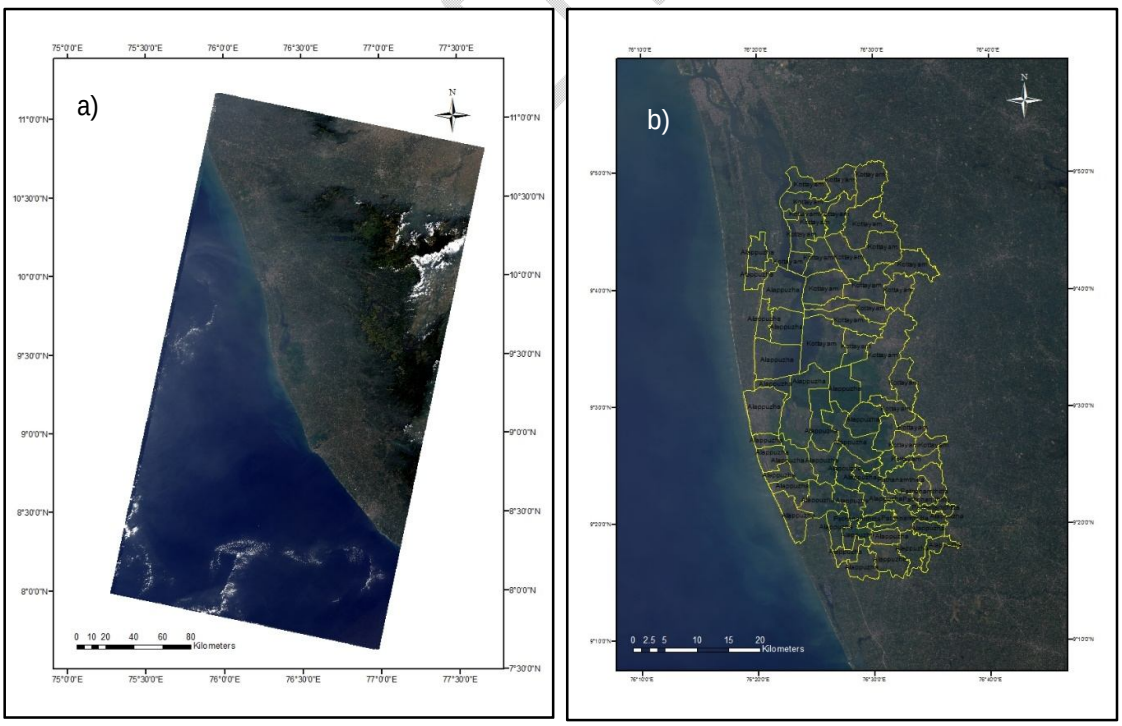

Fig.4 Mosaiked composite image (4a) and study area overlaid on composite image

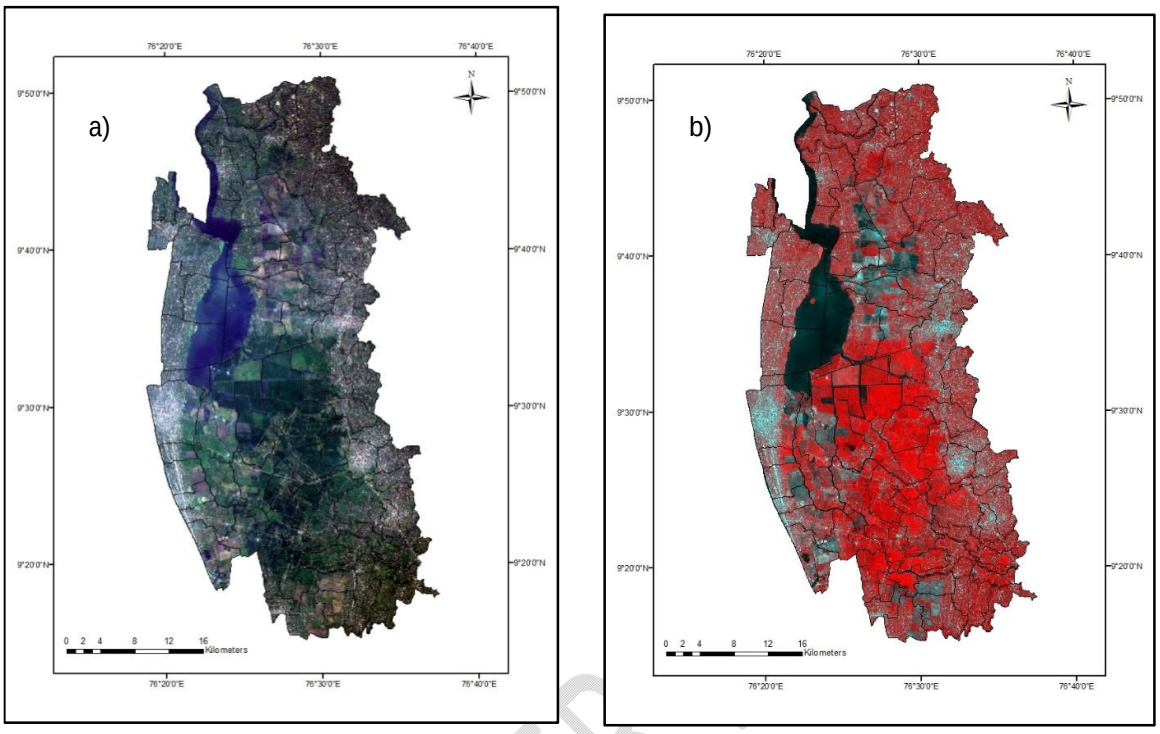

Fig.5 The clipped study area in True Colour Composite (5a) and False Colour Composite (5b)

such as paddy areas, other vegetation, low vegetation, built-up areas, and water bodies was found to be appropriate (Fig. 6a). The rice area was delineated by removing the classes like built-up areas, low vegetation, other vegetation, and water bodies (Fig. 6b). When a few classes are needed for analysis, supervised classification is employed. For the analyst to construct an appropriate signature from the image for classification. it is also necessary to have some prior knowledge of pixels in order to represent classes that you wish to extract from the image. Information regarding the land cover in the training sites was obtained by field visits and ground truthing.

3. Result and Discussion

Maps illustrating the land use patterns in Kerala's Kuttanad region were created with five distinct classes, as depicted in Fig. 6a. Fig. 6b presents the rice area map developed for Kuttanad and the estimated rice area is 43,550.28 ha. The areas of other classes were estimated as follows: other vegetation (22,989.22 ha), low vegetation (12,812.26 ha), urban areas or built-up structures (57,185.35 ha), water bodies (10,157.02 ha). The classification of Kuttanad region is summarized in Table 3. The overall rice area evaluated throughout the five blocks (43,550.28 ha),is marginally more than the actual acreage recorded in the Farm Guide (2023–24) for the *Puncha* season in 2021–22, which is 41,496.33 ha. By identifying between the rice and non-rice sectors, it was confirmed that the rice region

comprised 29.7% of the research area. To enhance accuracy, the remaining classifications without rice cultivation were grouped into a single category representing non-rice areas.

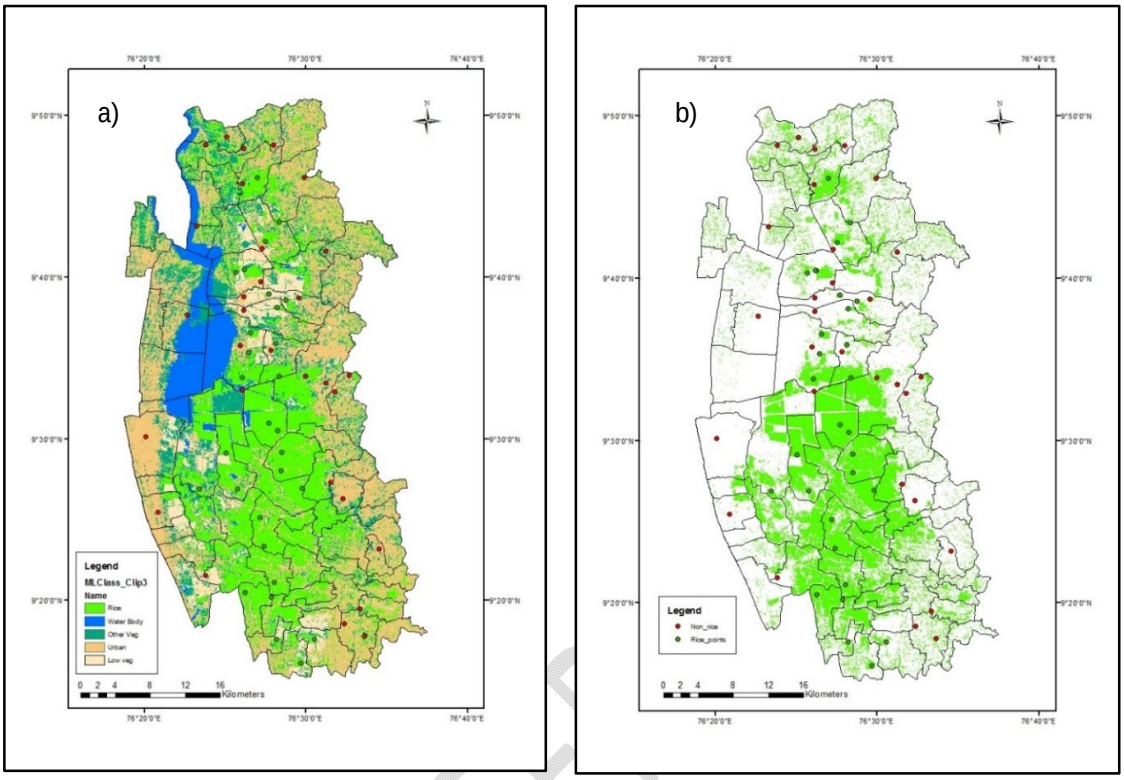

Fig.6 Classified image with 5 classes (6a) and rice area delineated with rice and non rice points (6b)

Fig 6b shows the 60 validation points distributed throughout the Kuttanad region, with 30 points for rice and 30 for non-rice. The Regions of Interest (ROIs) created using high-resolution Google Earth pictures and ground-truth data were compared to the rice area classification map. The findings indicate that there is a very high degree of agreement between the field data and the categorization map for rice. Using data from rice and non-rice areas, the classes that were defined and the actual land coverage were compared to create a confusion matrix and kappa coefficient that were used to assess accuracy. The accuracy of classification is summarized in Table 4. With a kappa coefficient of 0.87, the classification attained an average accuracy of 93.33%.

Several researchers have attempted area delineation in rice based on various optical satellite products the obstructions rendered Zhang et al. (2023) used Google Earth Engine (GEE) and Landsat images from 1990 to 2020 to create a Phenology-assisted Supervised Paddy Rice (PSPR) mapping framework in Heilongjiang Province, China, with a high degree of accuracy (R^2 = 0.993). Zhao et al. in 2021 obtained high-resolution multi-temporal vegetation indicators (NDVI, LSWI) and mapped paddy rice with an overall accuracy of 93% by combining Sentinel-2 and MODIS data. The difficulties caused by cloud cover in southwest China were successfully resolved by this technique.

Cao et al. (2021) mapped double- and single-cropping rice in Southern China

using Landsat time series data and a decision tree algorithm based on the Enhanced Vegetation Index (EVI). With accuracy ranging from 82% to 93%, they discovered that cloud-free photos taken during crucial growing seasons produced the most accurate results. An object-based approach combining merged MODIS and Landsat data coupled with phenological information was presented by Zhang and Lin (2019). Their technique worked well for mapping rice in cloudy areas, with an accuracy of 92.38%. These studies show that the supervised and object-based classification methods were quite successful at capturing the spatial heterogeneity of rice fields in areas that frequently experience cloud cover.

Using Sentinel-2 data, Raju et al. (2022) calculated the rice production areas in Kerala's Palakkad district and observed comparable results, with an average accuracy of 85% and a kappa coefficient of 0.72. Ajith et al. (2017) used Landsat 8 OLI images to study rice regions in the Thanjavur district of Tamil Nadu, and they found similar results with an accuracy of 87% and a kappa coefficient of 0.74. In another study, Kontgis *et al.*, (2015) looked into the mapping of rice paddies in Vietnam's Mekong River Delta, utilizing dense time series data from Landsat. Their approach achieved an impressive accuracy rate of over 90%, with omission and commission errors ranging from 6% to 25%. The research effectively differentiated between single, double, and triple-cropped rice paddies through a supervised classification that relied on various cropping pattern examples. Raza *et al.*, (2018) took advantage of Landsat 8 data and GIS technology to find appropriate sites for rice production in Pakistan's Punjab province. According to their research, 24.85% of the existing cultivated land was considered unsuitable and 6.8% of the area was rated as least suitable, both of which ultimately contributed to reduced production. Sethi et al. (2014) also determined the acreage of rice in Haryana using Landsat ETM+ data with ISODATA unsupervised classification. This study demonstrates how crop covering variability and planted area mapping might affect regional projections of water demand and production. The *Virippu* and *Mundakan* seasons in Kerala correspond to the southwest and northeast monsoons, respectively. In comparison to the *Mundakan* and *Puncha* seasons, the *Virippu* season has more cloud cover in satellite imagery due to the southwest monsoon's influence. Utilizing optical remote sensing to map rice lands is made possible by the *Puncha* season, which does not coincide with the monsoon and offers more cloud-free images. With supervised classification, rice areas were mapped and landforms were distinguished with high accuracy using Landsat 8 OLI pictures.

This study uses digital supervised classification based on FCC from Landsat 8 OLI Bands 1 to 7 to identify land cover, other agricultural forms, and existing rice crops during the *Puncha* season. Acreage estimation using optical satellite images is often complicated by cloud cover, so mono-temporal images with minimal cloud interference were utilized for this study. This study depicts the potential of using mono-temporal optical satellite images for accurate classification of rice area in Kuttanad, Kerala.

Table 3 Classification of the Kuttanad Region

Classes	Area (ha)
Rice	43,550.28
Other vegetation	22,989.22
Low vegetation	12,812.26
Urban areas or built-up structures	57,185.35
Water bodies	10,157.02

Table.4 Confusion matrix for accuracy assessment of rice classification

	Predicted class from the map			
	Class	Rice	Non-rice	Accuracy
	Rice	28	2	93.33
	Non rice	2	28	93.33
	Reliability	93.33%	93.33%	
Average accuracy		93.33%		
Average reliability		93.33%		
Kappa coefficient		0.87		

Conclusion

The objective of this research was to apply supervised classification to a total of two datasets from Landsat 8 OLI to ascertain the test site's area under rice cultivation and assess the method's accuracy. The method produced a classification accuracy of 93.33%. In the Kuttanad region, the *Puncha* season does not coincide with the monsoon season, resulting in a lower likelihood of cloud interference for optical images. However, it is essential to ensure that we have cloud-free temporal images for accurately delineating rice areas. Rice areas in the reproductive phase of Uma rice are specifically looked for for identification, as this is the period when optical satellite images free of clouds are most likely to be obtained. The goal of this demonstration is to show that Landsat 8 OLI mono-temporal optical datasets offer good overall accuracy for classifying land cover. To ensure food security, it is essential to understand the rice area around a month or two before harvesting.

Disclaimer (Artificial intelligence)

Author(s) hereby declare that NO generative AI technologies such as Large Language Models (ChatGPT, COPILOT, etc.) and text-to-image generators have been used during the writing or editing of this manuscript.

Reference

1. Agricultural Statistics 2021-22
2. Ahmed, M. and Ahmad, S., 2017. Climate variability impact on rice production: adaptation and mitigation strategies. *Quantification of climate variability, adaptation and mitigation for agricultural sustainability*, pp.91-111.
3. Ajith, K., Geethalakshmi, V., Raghunath, K. P., Pazhanivelan, S. & Panneerselvam, S. (2017). Rice acreage estimation in Thanjavur, Tamil Nadu using Landsat 8 OLIIMAG ES and GIS techniques. International Journal of Current Microbiology and Applied Sciences, 6(7), 2327-2335. doi.org/10.20546/ijcmas.2017.607.275 .
4. Bolton, K. D., Friedl, A. M., 2013. Forecasting crop yield using remotely sensed vegetation indices and crop phenology metrics. Agriculture and Forest Meteorology 15 (173), 74–84.
5. Cao, J., Cai, X., Tan, J., Cui, Y., Xie, H., Liu, F., Yang, L. and Luo, Y., 2021. Mapping paddy rice using Landsat time series data in the Ganfu

Plain irrigation system, Southern China, from 1988− 2017. *International Journal of Remote Sensing*, *42*(4), pp.1556-1576.

6. Chen, L. 2007. Uncertainties in rice yield estimation using remote sensing data. Ph. D. Thesis, Zhejiang University, Hangzhou Shi, Zhejiang Sheng, China.
7. Dong, J., Xiao, X., Menarguez, M.A., Zhang, G., Qin, Y., Thau, D., et al., 2016. Mapping paddy rice planting area in northeastern Asia with Landsat 8 images, phenology- based algorithm and Google Earth Engine. Remote Sens. Environ. 185, 142–154. https://doi.org/10.1016/j.rse.2016.02.016.
8. Erbek, F.S.,Özkan, C. and Taberner, M. 2004. International Journal of Remote Sensing. 25 : 1733-1748.
9. Genc, L., Inalpulat, M., Kizil, U. and Aksu. S. 2014. Determination of paddy rice field using Landsat 8 images. Int. Conference on Biol. Civil and Environ. Engi., (BCEE 2014) March 17-18, 2014 Dubai (UAE).
10. Goswami, S. B., Saxena, A. and Bairagi, G. D. 2012. Remote Sensing and GIS-based wheat crop acreage estimation of Indore district, M. P. Int. J. Emerg. Technol. Adv. Engi., 2(3).
11. Government of India. 2023. Agricultural statistics at a glance. New Delhi: Directorate of Economics and Statistics, Ministry of Agriculture and Farmers Welfare, Government of India. Available at: https://www.researchgate.net/publication/282467313_Comparing_System_of_Wheat_Intensification_SWI_with_standard_recommended_practices_in_the_north-western_plain_zone_of_India [accessed Oct 03 2024].
12. Government of Kerala. 2024. Farm Guide 2024. New Delhi: Thiruvananthapuram: Department of Agriculture and Department of Farmer's welfare, Government of Kerala. Available at: https://keralaagriculture.gov.in/wp-content/uploads/2024/02/Farmguide-2024.pdf [accessed Oct 03, 2024].
13. Hedayati, A., Vahidnia, M.H. and Behzadi, S., 2022. Paddy lands detection using Landsat-8 satellite images and object-based classification in Rasht city, Iran. *The Egyptian Journal of Remote Sensing and Space Science*, *25*(1), pp.73-84
14. Huang, J. F., Tang, S. C., Ousama, A. I., Wang, R. C., 2002. Rice yield estimation using remote sensing and simulation. J. Zhejiang Univ. - Sci. 3, 461–466.
15. Huke, R. E. and Huke, E. H. 1997. Rice area by type of culture: South, Southeast, and East Asia. A revised and updated database. International Rice Research Institute, Los Banos, Laguna, Philippines.
16. Jiang, Y., Dong, Y. and He, B., 2018, June. Large-area yield estimation method for rice using MODIS data production. In *2018 Fifth International Workshop on Earth Observation and Remote Sensing Applications (EORSA)* (pp. 1-3). IEEE.
17. John, A. Richards and Xiuping Jia, 2006. Remote Sensing Digital Image Analysis. 4th Edition, Springer-Verlag Berlin Heidelberg, Germany.
18. Karydas, C. G., Toukiloglou, P., Minakou, C., Gitas, I. Z., 2015. Development of a rule- based algorithm for rice cultivation mapping using Landsat 8 time series. In: Third International Conference on Remote Sensing and Geoinformation of the Environment (RSCy2015). https://doi.org/10.1117/12.2193162.

19. Khush, G. S., 2005. What it will take to Feed 5.0 Billion Rice consumers in 2030. Plant Mol. Biol. 59 (1), 1–6. https://doi.org/10.1007/s11103-005-2159-5.
20. Kontgis, C., Schneider, A. and Ozdogan, M., 2015. Mapping rice paddy extent and intensification in the Vietnamese Mekong River Delta with dense time stacks of Landsat data. *Remote Sensing of Environment*, *169*, pp.255-269.
21. Koppe, W., Gnyp, M. L., Hütt, C., Yao, Y., Miao, Y., Chen X. and Bareth, G. 2013. Rice monitoring with multi-temporal and dual polarimetric Terra SAR-X data. Int. J. Appl. Earth Observation and Geoinformation, 2: 568- 576.
22. Mansaray, L. R., Yang, L., Kabba, V. T. S., Kanu, A. S., Huang, J., Wang, F., 2019. Optimising rice mapping in cloud-prone environments by combining quad-source optical with Sentinel-1A microwave satellite imagery. GIScience Remote Sens. 56 (8), 1333–1354. https://doi.org/10.1080/15481603.2019.1646978.
23. Matsumura, M., Takeuchi, H., Satoh, M., Sanada-Morimura, S., Otuka, A., Watanabe, T., Thanh, D. V., 2009. Current Status of Insecticide Resistance in Rice Planthoppers in Asia. Planthoppers: New Threats to the Sustainability of Intensive Rice Production Systems in Asia, pp. 233–244.
24. Miranda, E., Mutiara, A., Ernastuti, B. and Wibowo, W. C. 2018. Classification of Land Cover from Sentinel-2 Imagery Using Supervised Classification Technique (Preliminary Study). International Conference on Infor mation Management and Technology (ICIMTech), Jakarta, 2018 pp. 69-74.
25. Mondal, S., Jeganathan, C., Sinha, N. K., Rajan, H., Roy, T., Kumar, P., 2014. Extracting seasonal cropping patterns using multi-temporal vegetation indices from IRS LISS-III data in Muzaffarpur District of Bihar, India. The Egyptian Journal of Remote Sensing and Space Science 17 (2), 123–134. https://doi.org/10.1016/j.ejrs.2014.09.002.
26. Muhsin, I. and Kadhim, M. 2017. Monitoring of south Iraq marshes using classification and change detection techniques. Iraqi Journal of Physics. 15 (33) : 78-86.
27. Nuarsa, I.W., Nishio, F., Hongo, C., 2012. Rice yield estimation using Landsat ETM data and field observation. J. Agric. Sci. 4 (3) https://doi.org/10.5539/jas.v4n3p45.
28. Persello, C., Tolpekin, V.A., Bergado, J.R. & de By, R.A. (2019). Delineation of agricultural fields in smallholder farms from satellite images using fully convolutional net works and combinatorial grouping. Remote Sensing of Environment, 231, 111253-111267. doi.org/10.1016/j.rse.2019.111253.
29. Raju, C., Ajith, K., Ajithkumar, B., Anitha, S. and Vijayan, V.D., 2022. Rice area mapping in Palakkad district of Kerala using Sentinel-2 data and Geographic information system technique. *Journal of Applied and Natural Science*, *14*(4), pp.1360-1366.
30. Raza, S.M.H., Mahmood, S.A. & Khan, A.A. (2018). Delineation of potential sites for rice cultivation through multi-criteria evaluation (MCE) using remote sensing and GIS. International Journal of Plant

Production, 12, 1-11. doi.org/10.1007/s42106-017-0001-z.
31. Roy, D.P., Wulder, M.A., Loveland, T.R., Woodcock, C.E., Allen, R.G., Anderson, M.C., Helder, D., Irons, J.R., Johnson, D.M., Kennedy, R., et al., 2014. Landsat-8: science and product vision for terrestrial global change research. Remote Sens. Environ. 145, 154–172.
32. Sethi, R.R., Sahu, A.S., Kaledhonkar, M.J., Sarangi, A., Rani, P., Kumar, A. & Mandal, K.G. (2014). Quantitative determination of rice cultivated areas using geospatial techniques. IOSR Journal of Environmental Science, Toxicology and Food Technology, 8(4), 76-81. http://www.iosrjournals.org/iosr-jestft/pages/8(4)Version-2.html
33. Shen, G. and Nie, C., 2023, July. Mapping Rice Area Using Sentinel-1 SAR Data and Deep Learning. In *IGARSS 2023-2023 IEEE International Geoscience and Remote Sensing Symposium* (pp. 3402-3405). IEEE.
34. Wang, J., Xiao, X., Qin, Y., Dong, J., Zhang, G., Kou, W., et al., 2015. Mapping paddy rice planting area in wheat-rice double-cropped areas through integration of Landsat-8 OLI, MODIS, and PALSAR images. Sci. Rep. 5 (1) https://doi.org/10.1038/srep10088.
35. Yang, X. H. 2007. Study on the remote sensing information extraction of rice based on neural network and support vector machine. Ph. D. Thesis, Zhejiang University, Hangzhou Shi, Zhejiang Sheng, China.
36. Yedage, A. S., Gavali, R. S. and Survanshi, A. 2013. Assessment of pomegranate orchard using remote sensing and GIS techniques for the Solapur, Maharashtra. Indian Streams Res. J., 3(3).
37. Yuan, S., Linquist, B.A., Wilson, L.T. *et al.* Sustainable intensification for a larger global rice bowl. *Nat Commun* **12**, 7163 (2021). https://doi.org/10.1038/s41467-021-27424-z
38. Zhang, C., Zhang, H. and Tian, S., 2023. Phenology-assisted supervised paddy rice mapping with the Landsat imagery on Google Earth Engine: Experiments in Heilongjiang Province of China from 1990 to 2020. *Computers and Electronics in Agriculture*, *212*, p.108105.
39. Zhang, H., Li, Q., Liu, J., Shang, J., Du, X., Zhao, L., et al., 2017. Crop classification and acreage estimation in North Korea using phenology features. GIScience Remote Sens. 54 (3), 381–406. https://doi.org/10.1080/15481603.2016.1276255.
40. Zhang, Meng, and Hui Lin. "Object-based rice mapping using time-series and phenological data." *Advances in Space Research* 63, no. 1 (2019): 190-202.
41. Zhao, R., Li, Y., Chen, J., Ma, M., Fan, L. and Lu, W., 2021. Mapping a paddy rice area in a cloudy and rainy region using spatiotemporal data fusion and a phenology-based algorithm. *Remote Sensing*, *13*(21), p.4400.
42. Zhao, R., Li, Y., Chen, J., Ma, M., Fan, L. and Lu, W., 2021. Mapping a paddy rice area in a cloudy and rainy region using spatiotemporal data fusion and a phenology-based algorithm. *Remote Sensing*, *13*(21), p.4400.